

The role of the dynamics of focal adhesion kinase in the mechanotaxis of endothelial cells

Song Li^{*†}, Peter Butler^{*}, Yingxiao Wang^{*}, Yingli Hu^{*}, Dong Cho Han[‡], Shunichi Usami^{*}, Jun-Lin Guan[‡], and Shu Chien^{*§}

^{*}Department of Bioengineering and The Whitaker Institute of Biomedical Engineering, University of California at San Diego, La Jolla, CA 92093-0427; and [‡]Department of Molecular Medicine, College of Veterinary Medicine, Cornell University, Ithaca, NY 14853

Communicated by Yuan-Cheng B. Fung, University of California at San Diego, La Jolla, CA, January 10, 2002 (received for review December 12, 2001)

The migration of vascular endothelial cells (ECs) is critical in vascular remodeling. We showed that fluid shear stress enhanced EC migration in flow direction and called this "mechanotaxis." To visualize the molecular dynamics of focal adhesion kinase (FAK) at focal adhesions (FAs), FAK tagged with green fluorescence protein (GFP) was expressed in ECs. Within 10 min of shear stress application, lamellipodial protrusion was induced at cell periphery in the flow direction, with the recruitment of FAK at FAs. ECs under flow migrated with polarized formation of new FAs in flow direction, and these newly formed FAs subsequently disassembled after the rear of the cell moved over them. The cells migrating under flow had a decreased number of FAs. In contrast to shear stress, serum did not significantly affect the speed of cell migration. Serum induced lamellipodia and FAK recruitment at FAs without directional preference. FAK(Y397) phosphorylation colocalized with GFP-FAK at FAs in both shear stress and serum experiments. The total level of FAK(Y397) phosphorylation after shear stress was lower than that after serum treatment, suggesting that the polarized change at cell periphery rather than the total level of FAK(Y397) phosphorylation is important for directional migration. Our results demonstrate the dynamics of FAK at FAs during the directional migration of EC in response to mechanical force, and suggest that mechanotaxis is an important mechanism controlling EC migration.

The migration of vascular endothelial cells (ECs) plays an important role in angiogenesis and postangioplasty wound healing. Cell migration is a coordinated process consisting of adhesion at the leading edge and detachment at the rear (1, 2). The focal adhesions (FAs), cytoskeleton, and signaling pathways that mediate cell migration need to respond to diverse extracellular signals and translate them into precisely regulated intracellular responses. There have been many studies on EC migration in response to gradients of soluble chemicals (chemotaxis) and immobilized extracellular matrix (haptotaxis; refs. 3–6). However, the effect of mechanical environment on EC migration is not well understood.

ECs are constantly subjected to shear stress, the tangential component of hemodynamic force caused by blood flow. It has been shown that shear stress induces EC monolayer remodeling, e.g., increase of stress fibers and alterations in gene expression (7, 8). Shear stress can modulate EC migration in wounding area and vascular stent surface (9–12), but the kinetics and molecular mechanism of EC migration in response to shear stress remain to be determined.

Integrins are transmembrane adhesion receptors that link the extracellular matrix to cytoskeletal proteins and signaling molecules at FAs (13–15). Integrin-matrix binding activates the signaling cascade at FAs to modulate cell migration (13, 14). Focal adhesion kinase (FAK) is a cytoplasmic tyrosine kinase that colocalizes with integrins at FAs. FAK mediates the FA dynamics and signaling in response to growth factors and integrin-ligand binding (16, 17). Phosphorylation of FAK at Tyr-397 [*p*-FAK(Y397)] upon cell adhesion allows FAK to associate with Src, which triggers downstream signaling events such as phosphorylation of mitogen-activated kinases, p130^{cas},

and paxillin to mediate cell adhesion and migration (18–24). Recent studies show that FAK is required for mechanosensing and persistent migration of fibroblasts (25, 26). We and others have shown that shear stress induces a transient activation of FAK in EC monolayer (27–29). These previous studies focused on the analysis of the global activity of FAK by using traditional biochemical assays; the subcellular distribution and dynamics of FAK at FAs and the role of this spatial dynamics in cell migration in response to mechanical and chemical stimuli remain to be determined.

Here, we defined the kinetics of shear stress-induced directional migration of ECs. By expressing green fluorescence protein (GFP)-tagged FAK, we demonstrated the molecular dynamics of FAK at FAs in migrating ECs in response to shear stress and serum. The results showed that *p*-FAK(Y397) was correlated with FAK dynamics at FAs. Our findings indicate that the spatial dynamics of signaling at FAs is critical in directional migration, and that mechanotaxis is an important mechanism controlling EC migration.

Materials and Methods

Cell Culture. Cell culture reagents were obtained from GIBCO/BRL. Bovine aortic ECs (BAECs) before passage 10 were maintained in DMEM supplemented with 10% (vol/vol) FBS. All cell cultures were maintained in a humidified 5% CO₂/95% air incubator at 37°C. Before cell seeding, glass slides were coated with fibronectin (1 μg/cm²) for 2 h and blocked with 1% BSA for 30 min. BAECs were seeded on fibronectin-coated slides in DMEM containing 0.5% serum for 3 h at ≈10% confluence; they were subjected to shear stress, stimulated with 10% serum in DMEM, or kept as static control.

Flow System. A circulation flow system (30) was used to impose shear stress on cultured ECs at 37°C. The slide with subconfluent BAECs was mounted in a rectangular flow channel created by sandwiching a silicone gasket (0.015-cm thick) between the slide and an acrylic plate. Laminar shear stress was generated by the flow resulting from the hydrostatic pressure difference between two reservoirs. The shear stress applied was 12 dyn/cm², a level found in arteries and capillaries.

DNA Constructs and Transfection. GFP-actin was obtained from CLONTECH. To construct GFP-FAK, the cDNA encoding FAK was excised from pBS-FAK (gift of J. Thomas Parsons, Univ. of Virginia, Charlottesville) by digestion with *Sma*I and *Sal*I and inserted into pEGFP-c3 (CLONTECH). DNA plasmids

Abbreviations: EC, endothelial cell; FA, focal adhesion; FAK, focal adhesion kinase; GFP, green fluorescence protein; BAEC, bovine aortic endothelial cell; *p*-FAK(Y397), phosphorylation of FAK at tyrosine residue 397; V_x, velocity in X direction; V_y, velocity in Y direction.

[†]Present address: Department of Bioengineering, University of California, Berkeley, CA 94720-1762.

[§]To whom reprint requests should be addressed. E-mail: schien@bioeng.ucsd.edu.

The publication costs of this article were defrayed in part by page charge payment. This article must therefore be hereby marked "advertisement" in accordance with 18 U.S.C. §1734 solely to indicate this fact.

were transfected into ECs by using GenePorter reagent (GeneSystems, San Diego, CA). ECs were used for experiments 2 days after transfection.

Time-Lapse Microscopy. Cell migration was monitored by time-lapse microscopy with a Nikon inverted microscope with 10× objective. Phase contrast images were collected with a Hamamatsu charge-coupled device camera at 10-min intervals and transferred from a frame grabber to computer storage. Dynamic motion of individual cells was analyzed by using Dynamic Image Analysis System software (Solltech, Oakdale, IA).

The dynamics of GFP proteins were monitored by time-lapse confocal microscopy with a Nikon inverted microscope (40× oil objective) and a Bio-Rad MRC 1024 laser scanning confocal imaging system. GFP was excited at 488 nm and detected between 506 and 538 nm. The dynamics of FAs were individually tracked and analyzed with a program written in Labview G programming language (National Instruments, Austin, TX). After background subtraction, the images were thresholded, and FAs were tracked by a modified nearest-neighbor algorithm for calculation of the position, number, and area of FAs.

Immunostaining and Confocal Microscopy. BAECs were fixed in 4% (wt/vol) paraformaldehyde, permeabilized in 0.5% Triton X-100, and stained with a monoclonal anti-*p*-FAK(Y397) antibody (BD Transduction Laboratories, Lexington, KY), which was detected with an anti-mouse antibody conjugated with Cy5. Actin cytoskeleton was stained with rhodamine-conjugated phalloidin. Stained samples were examined by using Zeiss LSM510 confocal microscopy system with 100× oil objective. An image of a 1- μ m thick section was collected at the bottom of the cell for each field. GFP, rhodamine, and Cy5 were excited at 488, 543, and 633 nm and detected at 505–530, 560–615, and >650 nm, respectively. The images were acquired under the same conditions for each experiment. The intensity of fluorescence signals was quantified with NIH IMAGE software.

Results

Shear Stress, but Not Serum, Induced Directional Migration of ECs. We first characterized the modulation of BAEC migration by shear stress as a function of time. We also treated BAECs with serum, which has been shown to regulate cytoskeleton and cell adhesion (31). BAECs at 10% confluency were subjected to shear stress, stimulated with serum, or kept as static control. The migration speed and its projections in directions parallel (V_x) and perpendicular (V_y) to the long axis of the channel (X -direction) were calculated from the time-lapse phase contrast microscopy (Fig. 1). Under static conditions, ECs showed random migration without any preferential direction (Fig. 1A). Serum did not significantly affect EC migration. The application of shear stress for 1 h, however, caused >90% of cells to migrate in the flow direction. We use “mechanotaxis” to describe the directional migration of cells induced by mechanical forces, analogous to chemotaxis and haptotaxis. Application of shear stress in a direction opposite to that of the migration of a cell caused the cell to change its direction and migrate along the flow direction (Fig. 1B). Shear stress caused lamellipodial protrusion in the flow direction (in 0.5 h), leading to a gradual turning of the cell body (in 1 h). The effects of shear stress on the temporal change of cell migration speed (regardless of direction) are shown in Fig. 1C. After 30 min of shearing, the migration speed increased by 50% above the preshear value ($P < 0.05$). Shear stress caused the absolute value of velocity in the X direction ($|V_x|$) to increase significantly over that under static conditions, with a peak of +70% at 30 min and a plateau of about +30% at 1–2 h ($P < 0.05$). The average V_x (with directional signs taken into account) increased from 0 (random directions of migration) to a positive

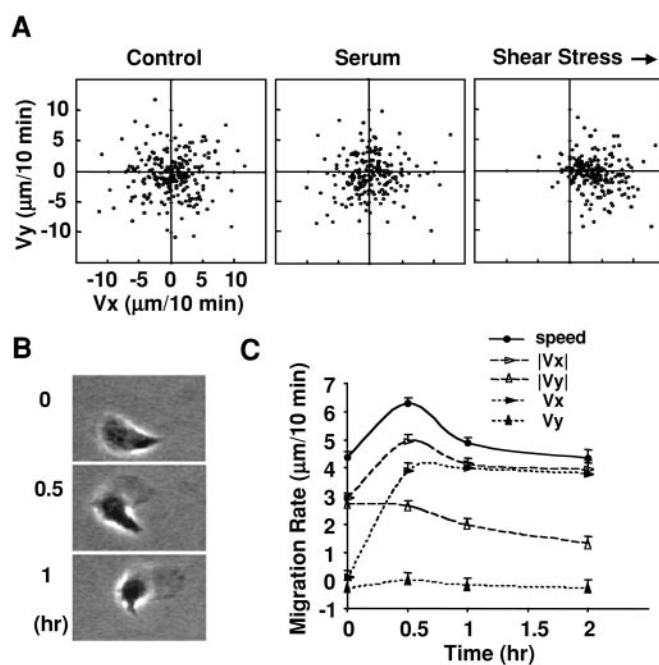


Fig. 1. Modulation of EC migration by shear stress and serum. BAECs were plated on fibronectin-coated slides for 3 h in DMEM with 0.5% serum. The ECs were subjected to fluid shear stress, treated with 10% serum, or kept as control. EC migration was monitored by phase contrast microscopy at 10-min intervals for 2 h. The migration speed and its projections in the longitudinal direction of the flow channel (X) and the perpendicular direction (Y) were determined from the positions of cell centroids. The flow direction was from left to right in the X direction. (A) The speed in X (V_x) and Y (V_y) directions of a cell after 1 h of experiment (or control) was plotted in the V_x - V_y plane as a dot. Data were obtained by analyzing the migration of 100 cells pooled from three separate experiments. (B) Phase contrast images of a cell from a time-lapse recording after applying shear stress (0, 0.5, and 1 h). (C) Temporal changes of the EC migration rate.

value in the flow direction (+4 $\mu\text{m}/10$ min) after 30 min of shearing. The convergence of $|V_x|$ and V_x after 1 h of shearing indicates that the migration was predominantly in the X -direction. The average V_y did not change significantly, and the average $|V_y|$ decreased slightly after 1 h ($P < 0.05$). These results suggest that shear stress modulates both the rate and direction of EC migration, and that shearing for 1 h or longer increases migration in the flow direction while suppressing that in the perpendicular direction.

Shear Stress-Induced Polarized Recruitment of FAK at New FAs and Polarized Actin Polymerization. To visualize the dynamics of FAK and FAs during shear stress-induced cell migration, GFP-FAK was expressed in BAECs and its dynamics was monitored by confocal microscopy. Fig. 2A shows a cell migrating in the perpendicular direction before flow. The application of shear stress induced lamellipodial protrusions at the cell periphery within 2 min (arrows in Fig. 2A) without a preferential direction. By 10 min, FAK was recruited to FAs under the lamellipodial protrusion in the flow direction (arrows in Fig. 2A, 10 min). These new FAs provided attachment points for the lamellipodium for its stepwise protrusion in the flow direction. In contrast, the lamellipodia in the other directions had no such focal adhesion support and underwent retraction. There was no significant movement of preexisting FAs within the first 10 min of shearing, suggesting that shear stress did not move the FAs simply by mechanical pushing.

We expressed GFP-actin in BAECs to visualize the dynamics of actin in the shear-induced lamellipodial protrusion. As shown

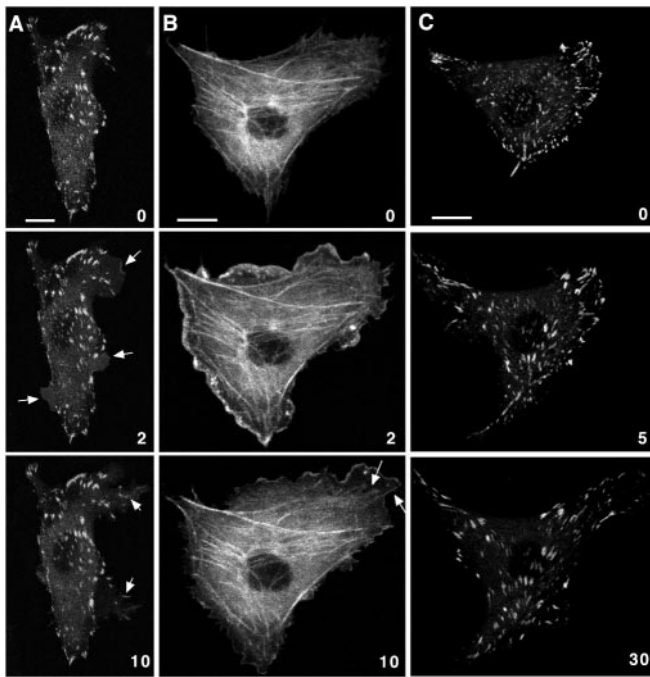


Fig. 2. Formation of focal adhesions stimulated by shear stress and serum at the early stage. BAECs expressing GFP-FAK or GFP-actin were subjected to shear stress or treated with serum as in Fig. 1. The flow direction was from left to right. The dynamics of GFP-FAK or GFP-actin were monitored by time-lapse confocal microscopy. (A) Fluorescence images of GFP-FAK taken at 0, 2, and 10 min after applying shear stress. (B) Fluorescence images of GFP-actin taken at 0, 2, and 10 min after applying shear stress. (C) Fluorescence images of GFP-FAK taken at 0, 5, and 30 min after serum stimulation. (Bars = 10 μm .)

in Fig. 2B, shear stress induced the formation of lamellipodia in all directions at the cell periphery within 2 min, and these lamellipodia waved around and were not stable. These results suggest that cell membrane extension is the first cell motion in response to shear stress. After 10 min of shearing, lamellipodial protrusion in the flow direction was stabilized by the polymerization of actin filaments (arrows in Fig. 2B, 10 min), whereas lamellipodia in other directions were either waving or retracting. These findings on the polarized lamellipodial protrusion, together with the results from Fig. 2A, suggest that shear stress can induce the formation of polarized FAs and the polymerization of actin filaments in the flow direction to support the persistent lamellipodial protrusion.

Serum also stimulated the formation of lamellipodia and FAs within minutes (Fig. 2C), but the lamellipodia extended in many directions throughout the period of observation, and the cells usually showed a multipolar shape and increased spreading (see Movie 1, which is published as supporting information on the PNAS web site, www.pnas.org). These morphological findings may explain why serum did not significantly affect cell migration speed (Fig. 1A).

Shear Stress-Induced Remodeling of Existing FAs for Directional Migration. After the initial phase of polarized lamellipodial protrusion, ECs under flow started the remodeling (movement, merging, or disappearance) of FAK at FAs to allow the cell body to turn toward the flow direction. Fig. 3 shows that a cell initially migrating against the flow turned into the flow direction under continuous shear stress. FAK was recruited to FAs at the front of the lamellipodium and the cell periphery by 30 min (arrow in Fig. 3). After 60 min of shearing, the polarity of the cell was more prominent, with more new FAs formed at the leading edge of the

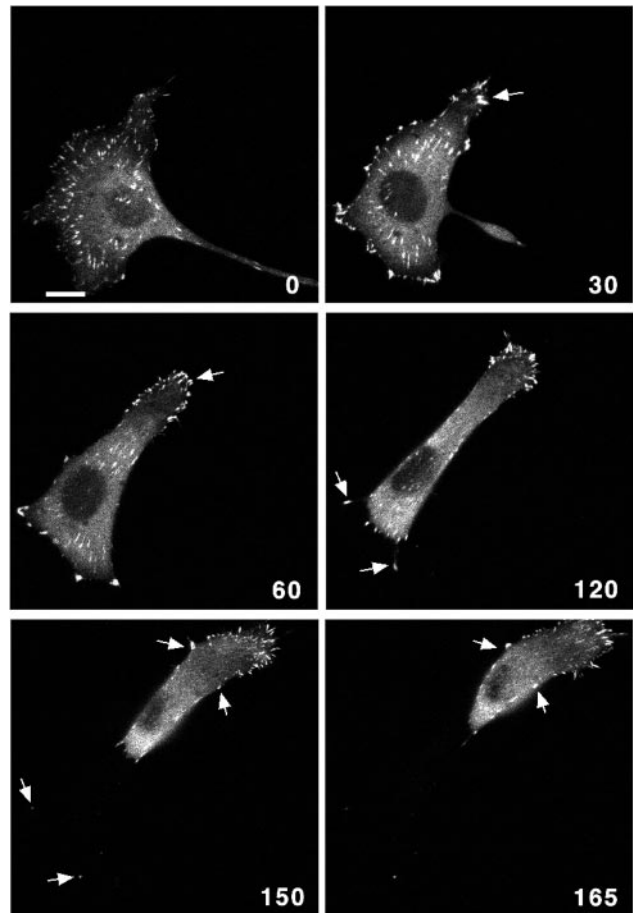


Fig. 3. Remodeling of FAs stimulated by shear stress. As in Fig. 2, BAECs expressing GFP-FAK were subjected to shear stress (from left to right). The dynamics of GFP-FAK were monitored by time-lapse confocal microscopy. Fluorescence images were taken at 0, 30, 60, 120, 150, and 165 min after applying shear stress. (Bar = 10 μm .)

cell (arrow in Fig. 3, 60 min), whereas no new FA formed in the central region of the cell. The preexisting FAs in the central region moved, merged, or disappeared, resulting in a decrease in number and increase in size (see Movie 2, which is published as supporting information on the PNAS web site; also, see quantitation in next section). These results suggest that the central region remodels its preexisting FAs, rather than forming new FAs, to adapt to the change of mechanical environment. FAK at the cell tail either became separated from the cell or disassembled. As shown in Fig. 3 (arrows at bottom left, 120 and 150 min), FAK detached from the cell tail and remained with the substratum. Cell detachment at the rear seemed to facilitate lamellipodial protrusion in the front, with a concurrent increase in new FA formation (see Movie 2). Forward movement of the lamellipodia was restrained until the rear part of the cell retracted (Fig. 3, 120 min).

After the remodeling phase, cells entered a phase of persistent migration under flow, indicating an adaptation to the new mechanical environment. The distribution of FAK was highly polarized, being recruited only to FAs at the leading edge. These newly formed FAs did not grow in size (see Movie 2); they either dissembled shortly or remained stationary until passed over by the cell body (arrows at top right in Fig. 3, 150 and 165 min) and then dissembled.

Quantitative Analysis of Shear Stress- and Serum-Induced FA Remodeling. To quantify the remodeling of FAK at FAs, we tracked the movement of individual FAs, and determined the

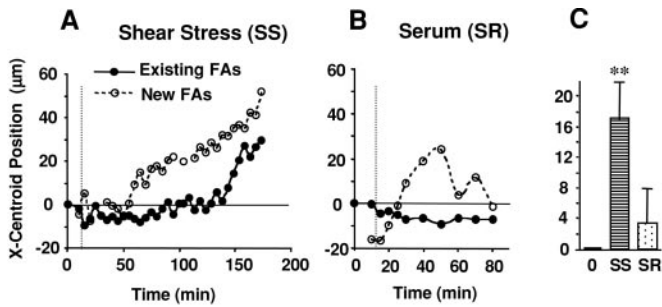


Fig. 4. The X-centroid position of FAs in response to shear stress and serum. The dynamics of FAs were tracked in shear stress and serum experiments, and the X-centroid positions of FAs were calculated. The longitudinal direction of the flow channel was defined as the X direction. The origin of the X and Y coordinates was chosen at the average X centroid position of the FAs in the cell at the beginning of the experiments. (A) Average of the X centroids of existing and new FAs (in Fig. 3) under shear stress. (B) Average of the X centroids of existing and new FAs (in Fig. 2C) after serum stimulation. (C) Statistical analysis of average X-centroid position of new FAs within the first hour after shear stress or serum stimulation. In A and B, filled circles represent the results for existing FAs in each frame. Open circles represent the results for new FAs in each frame. The vertical dotted lines indicate the time when shear stress or serum was applied to the cell. In C, bars represent means \pm SE (at least three cells). *, statistical significance ($P < 0.05$) compared with that at $t = 0$. **, statistical significance ($P < 0.05$) compared with that at $t = 0$ and within the first hour of serum stimulation.

position, number, and area of FAs. The results for the cells in Figs. 3 and 2C are shown in Figs. 4 and 5 as representative examples for treatments with shear stress and serum, respectively. Fig. 4A shows the position of the average X-centroid

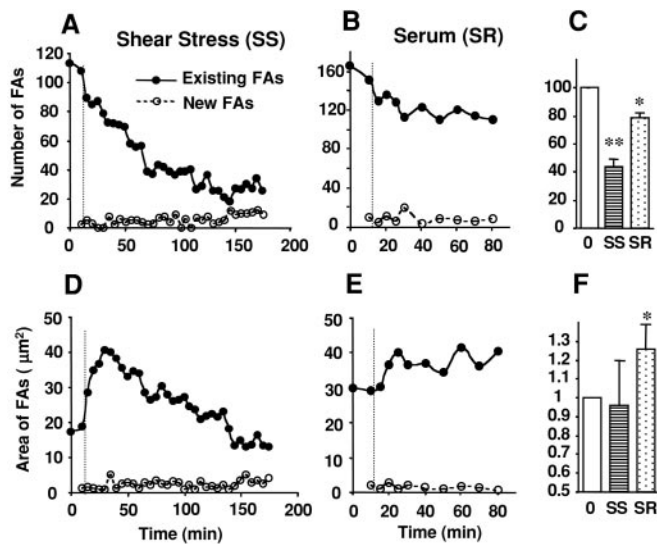


Fig. 5. The number and area of FAs in response to shear stress and serum. The dynamics of FAs was tracked in shear stress and serum experiments, and the number and area of FAs were calculated. (A) Average of the number of existing and new FAs (in Fig. 3) under shear stress. (B) Average of the number of existing and new FAs (in Fig. 2C) after serum stimulation. (C) Statistical analysis of the total number of FAs after 1 h of shear stress or serum stimulation. The number of FAs was normalized with the cell number at the beginning of the experiment ($t = 0$). (D) Average of the area of existing and new FAs (in Fig. 3) under shear stress. (E) Average of the area of existing and new FAs (in Fig. 2C) after serum stimulation. (F) Statistical analysis of the total area of all FAs after 1 h of shear stress or serum stimulation. The area was normalized with the total area at $t = 0$. Other figure legends are the same as in Fig. 4, except that ** denotes statistical significance ($P < 0.05$) compared with that at $t = 0$ and after 1 h of serum stimulation.

position of FAs (positive values indicate a motion in the X-direction, i.e., in the direction of flow). In these figures, the “new FAs” refer to the FAs that appeared during the most recent period; all others are designated as “existing FAs,” which include the FAs formed in the preceding period. Comparison of the curves for new and existing FAs showed that the X-centroid values were greater for the new FAs induced by shear stress, indicating that they were located preferentially in the front part of the cell. In contrast, the X centroids of new FAs fluctuated after serum stimulation, implying that they formed in different directions (Fig. 4B). Statistical analysis of new FAs formed within the first hour of stimulation showed that shear stress induced new FAs preferentially in the flow direction, but serum did not (Fig. 4C).

Both shear stress (Fig. 5A) and serum (Fig. 5B) decreased the total number of FAs. After 1 h, shear stress decreased the total number of FAs ($\approx -60\%$) more than serum stimulation ($\approx -20\%$; Fig. 5C), suggesting that shear stress induces a faster FA disassembly. Both shear stress and serum increased total areas of FAs (Fig. 5D and E), which would enhance cell adhesion. Together, these data indicate that the FAs became larger after the application of shear stress and serum. The shear stress induced a transient increase in total FA area, which later decreased with the faster disassembly of FAs. In contrast, serum caused a sustained increase in total FA area, which was maintained at a plateau of $\approx +25\%$ over control (Fig. 5F).

FAK(Y397) Phosphorylation Correlated with the Recruitment of FAK to FAs.

The effects of shear stress and serum on *p*-FAK(Y397) distribution in BAECs are shown in Fig. 6 (pseudocolored red). The spatial distribution of *p*-FAK(Y397) shows excellent correlation with GFP-FAK (pseudocolored green) in BAECs under shear stress, serum treatment, as well as control states, as shown by the yellow or white colors in Fig. 6A–E and by the enlarged images (Fig. 6F–I). Thus, the recruitment of GFP-FAK at FAs could be used as an index of *p*-FAK(Y397). Application of shear stress for 10 min induced lamellipodial protrusion in flow direction (arrows in Fig. 6B), and this protrusion was accompanied by FAK recruitment and *p*-FAK(Y397) phosphorylation at the new FAs in lamellipodia. After 3 h of shearing, the cells turned into the flow direction (Fig. 6C). The FAs at the cell tail had less connection with stress fibers; this decrease in connection may facilitate tail detachment as the cell migrated under flow. In contrast, serum stimulation induced new FAs and *p*-FAK(Y397) in many directions (Fig. 6D). After 3 h of serum stimulation, the cells had larger FAs and more stress fibers (Fig. 6E). The total *p*-FAK(Y397) level after serum stimulation was 1.63 ± 0.23 fold ($n = 5$, $P < 0.05$) of that induced by shear stress.

New FAs under lamellipodia were usually small, and *p*-FAK(Y397) (Fig. 6F) had the same pattern as GFP-FAK (Fig. 6G). In the central portions of large FAs ($\approx 2 \mu\text{m}^2$), where actin filaments anchored, there was no detectable staining of either *p*-FAK(Y397) (arrows, Fig. 6H) or FAK (data not shown), suggesting the absence of FAK at the actin filament anchorage points at large FA complexes.

Discussion

We have studied the kinetics of directional EC migration in response to shear stress (Fig. 1) and the molecular dynamics of FAK at FAs during this mechanotaxis. The FA dynamics in response to shear stress consists of three phases. The first phase lasts for ≈ 10 min. It starts with random membrane spreading, which is followed by lamellipodial protrusion and new FA formation in the leading edge without significant movement of preexisting FAs (Fig. 2). The second phase is FA remodeling which may take hours, depending on FA distribution and cell orientation. The preexisting FAs merge, move, and/or disappear. The third phase is the persistent migration of ECs under

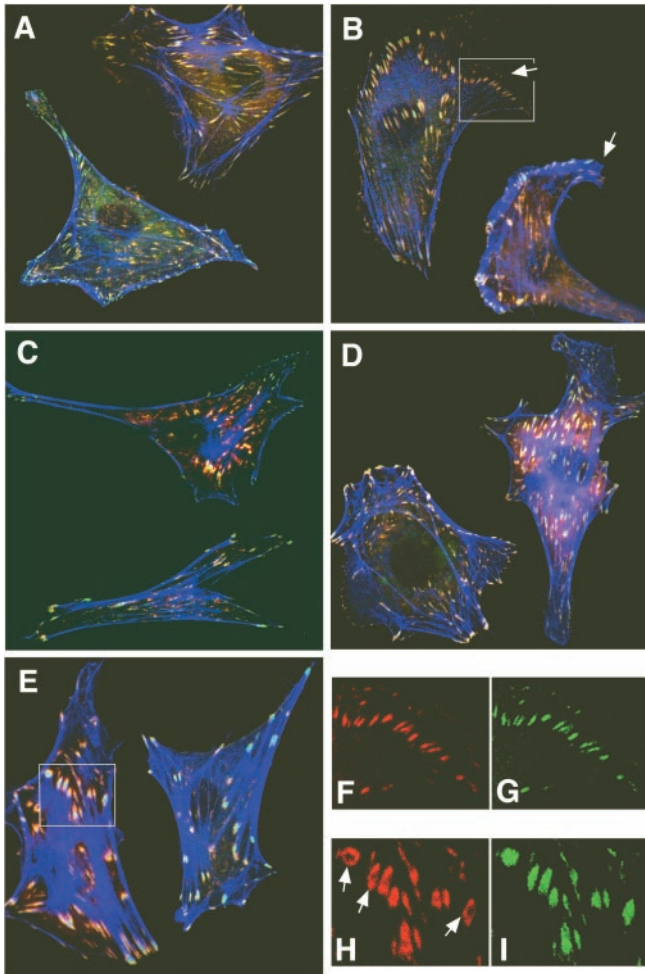


Fig. 6. Distribution of FAK(Y397) phosphorylation, GFP-FAK, and actin cytoskeleton. BAECs were subjected to shear stress (from left to right) or serum stimulation for 10 min or 3 h. The cells were stained for *p*-FAK(Y397) (pseudocolored red) and actin (pseudocolored blue). GFP-FAK was pseudocolored green. The pixels show yellow when green and red overlap and show white when green, red and blue all overlap. (A) Cells in 0.5% serum. (B) Cells subjected to shear stress for 10 min. (C) Cells subjected to shear stress for 3 h. (D) Cells stimulated with serum for 10 min. (E) Cells stimulated with serum for 3 h. (F and G) Enlarged portions of B with *p*-FAK(Y397) staining and GFP-FAK respectively. (H and I) Enlarged portions of E with *p*-FAK(Y397) staining and GFP-FAK respectively. (Bar = 10 μ m.)

flow. New FAs form at the leading edge, and either turn over quickly or remain stationary until the cell body glides over them (Fig. 3). Smilenov *et al.* found that FAs were stationary in migrating cells but motile in stationary cells (32). Our data showed that mechanotaxis involved both phenotypes. The movement of FAs in our stationary cells occurs when they remodel their FAs and change the migration direction (second phase of mechanotaxis), and this change in direction is probably related to the contraction of actin fibers, as reported in ref. 32.

The formation of new FAs in the flow direction is a key event in mechanotaxis. There are several possible explanations for the mechanisms of the polarized attachment of lamellipodia. One is that shear stress may cause polarized transport in the flow direction because of regional changes in membrane tension. The EC membrane has local high membrane curvature in resting state (33). Shear stress may unfold the membrane and cause the initial random spreading of cell membrane, followed by directional membrane movement, cytoplasm flow, and transport of

receptors and signaling molecules. Although there is no report on the shear-induced intracellular transport, it has been shown that shear stress can increase membrane fluidity in EC monolayer (34, 35). Alternatively, shear stress may produce a polarized mechanical microenvironment, which induces polarized subcellular activation of mechano-chemical signaling events such as actin polymerization and integrin activation. We have shown that shear stress can induce integrin activation (36, 37). It will be interesting to determine the subcellular distribution of activated integrins.

Shear stress not only induces new FAs at the leading edge but also enhances the disassembly of existing FAs. The number of FAs decreased significantly in ECs migrating under flow (Fig. 5). The rear detachment of a migrating cell facilitates the formation of new FAs at the leading edge (see Movie 2). The decrease of adhesions at the rear may break the balance of traction forces between the leading edge and the rear, thus generating a polarized driving force to promote lamellipodial protrusion and new FA formation in the flow direction. FAK disassembled at FAs could either recycle in cells or segregate from the cells and remain with the substratum (Fig. 3). This observation indicates that not only the transmembrane receptors (e.g., integrins; refs. 38 and 39), but also cytoplasmic signaling molecules at FAs (e.g., FAK) could segregate from the cells. This observation is consistent with the recent report that shear stress activates *m*-calpain and decreases FAK at FAs (40).

The exact role of FAK in FA dynamics (i.e., assembly or turnover) is controversial. Although FAK activation is accompanied by cell adhesion, FAK knock-out fibroblasts have increased number of FAs but reduced migration rate (41). Our time-lapse observation showed that FAK was recruited to new FAs to support lamellipodial protrusion and disappeared at the rear of cells (Figs. 2 and 3). These data suggest that FAK is involved in the assembly of FAs. The phenotype in FAK knockout cells could be attributed to the compensation of other pathways involved in FA assembly (42).

It has been shown that FAK phosphorylation is required for cell migration (18–25). In the present study, shear stress induced polarized FAK recruitment and *p*-FAK(Y397) phosphorylation at FAs in the leading edge (Figs. 3 and 6). In contrast, serum stimulation did not induce any changes with direction preference, although there was a high level of induced *p*-FAK(Y397). These results suggest that the polarized change of *p*-FAK(Y397) at the cell periphery, rather than the total level of *p*-FAK(Y397) *per se*, is necessary for effective directional migration. This suggestion might explain the recent finding by Wang *et al.* that overexpression of negative mutant FAK(Y397F), which interferes with the downstream signaling of endogenous *p*-FAK(Y397), did not affect fibroblast migration toward a more rigid substrate (26). On the other hand, the total level of *p*-FAK(Y397) may be more relevant to functions such as the regulation of gene expression and cell proliferation.

Mechanotaxis may be a general phenomenon operative in other types of cells. For example, we have shown that a mechanical force of 0.003 dyn can counter or reverse the chemotaxis migration of a polymorphonuclear leukocyte in a micropipette (43). The threshold of shear stress needed to induce mechanotaxis may depend on many factors such as cell types, adhesion strength, and the composition and activity of intracellular signaling molecules.

The remodeling of FAs and cytoskeleton in nonconfluent ECs and EC monolayer shares some common features, but there are also differences. Shear stress increases the size and decreases the number of FAs in both nonconfluent ECs (Figs. 3–5) and EC monolayers (44). However, shear stress induces polarized FAs at the downstream end of the nonconfluent ECs (Fig. 3), although it induces a polarized distribution of α β 3 integrin at the upstream end of the ECs in a monolayer (45). Shear stress

decreases stress fibers to enhance the migration of nonconfluent ECs (Fig. 6), but it increases stress fibers in EC monolayers to enhance anchorage (46, 47). These differences may be attributed to the constraint of EC migration in monolayer by cell–cell interactions vs. the relative lack of constraint for the migration of nonconfluent ECs. These results suggest that ECs can adapt to the mechanical environment in different manners to fulfill their functional needs.

The role of mechanical forces in FA dynamics during EC migration has important implications in EC wound healing and angiogenesis. In large vessels where convection is strong, mech-

anotaxis may have a more significant effect than chemotaxis. In the microcirculation, mechanotaxis may guide EC migration in angiogenesis during wound repair. Our results demonstrate the molecular dynamics of cell migration in response to shear stress and suggest that, in addition to chemotaxis and haptotaxis, mechanotaxis is an important mechanism controlling EC migration.

This research was supported in part by Research Grants HL-19454, HL-43026, and HL-64382 (to S.C.) and a Grant from the American Heart Association (to S.L.).

1. Lauffenburger, D. A. & Horwitz, A. F. (1996) *Cell* **84**, 359–369.
2. Sheetz, M. P., Felsenfeld, D., Galbraith, C. G. & Choquet, D. (1999) *Biochem. Soc. Symp.* **65**, 233–243.
3. Castellot, J. J., Jr., Karnovsky, M. J. & Spiegelman, B. M. (1982) *Proc. Natl. Acad. Sci. USA* **79**, 5597–5601.
4. Bowersox, J. C. & Sorgente, N. (1982) *Cancer Res.* **42**, 2547–2551.
5. Herbst, T. J., McCarthy, J. B., Tsilibary, E. C. & Furcht, L. T. (1988) *J. Cell Biol.* **106**, 1365–1373.
6. Stokes, C. L., Rupnick, M. A., Williams, S. K. & Lauffenburger, D. A. (1990) *Lab. Invest.* **63**, 657–668.
7. Davies, P. F. (1995) *Physiol. Rev.* **75**, 519–560.
8. Chien, S., Li, S. & Shyy, Y. J. (1998) *Hypertension* **31**, 162–169.
9. Ando, J., Nomura, H. & Kamiya, A. (1987) *Microvasc. Res.* **33**, 62–70.
10. Sprague, E. A., Luo, J. & Palmaz, J. C. (1997) *J. Vasc. Interv. Radiol.* 83–92.
11. Tardy, Y., Resnick, N., Nagel, T., Gimbrone, M. J. & Dewey, C. J. (1997) *Arterioscler. Thromb. Vasc. Biol.* **17**, 3102–3106.
12. Hsu, P.-P., Li, S., Li, Y.-S., Shunichi Usami, S., Ratcliffe, A., Wang, X. & Chien, S. (2001) *Biochem. Biophys. Res. Comm.* **285**, 751–759.
13. Hynes, R. O. (1992) *Cell* **69**, 11–25.
14. Sastry, S. K. & Horwitz, A. F. (1993) *Curr. Opin. Cell Biol.* **5**, 819–831.
15. Schwartz, M. A., Schaller, M. D. & Ginsberg, M. H. (1995) *Annu. Rev. Cell Dev. Biol.* **11**, 549–599.
16. Cary, L. A., Han, D. C. & Guan, J. L. (1999) *Histol. Histopathol.* **14**, 1001–1009.
17. Schlaepfer, D. D., Hauck, C. R. & Sieg, D. J. (1999) *Prog. Biophys. Mol. Biol.* **71**, 435–478.
18. Burridge, K., Turner, C. E. & Romer, L. H. (1992) *J. Cell Biol.* **119**, 893–903.
19. Schlaepfer, D. D., Hanks, S. K., Hunter, T. & van der Geer, P. (1994) *Nature (London)* **372**, 786–791.
20. Chen, Q., Kinch, M. S., Lin, T. H., Burridge, K. & Juliano, R. L. (1994) *J. Biol. Chem.* **269**, 26602–26605.
21. Zhu, X. & Assoian, R. K. (1995) *Mol. Biol. Cell* **6**, 273–282.
22. Vuori, K. & Ruoslahti, E. (1995) *J. Biol. Chem.* **270**, 22259–22262.
23. Gilmore, A. P. & Burridge, K. (1996) *Structure (London)* **4**, 647–651.
24. Cary, L. A., Han, D. C., Polte, T. R., Hanks, S. K. & Guan, J. L. (1998) *J. Cell Biol.* **140**, 211–221.
25. Gu, J., Tamura, M., Pankov, R., Danen, E. H., Takino, T., Matsumoto, K. & Yamada, K. M. (1999) *J. Cell Biol.* **146**, 389–403.
26. Wang, H.-B., Dembo, M., Hanks, S. K. & Wang, Y.-L. (2001) *Proc. Natl. Acad. Sci. USA* **98**, 11295–11300.
27. Ishida, T., Peterson, T. E., Kovach, N. L. & Berk, B. C. (1996) *Circ. Res.* **79**, 310–316.
28. Takahashi, M. & Berk, B. C. (1996) *J. Clin. Invest.* **98**, 2623–2631.
29. Li, S., Kim, M., Hu, Y. L., Jalali, S., Schlaepfer, D. D., Hunter, T., Chien, S. & Shyy, J. Y. (1997) *J. Biol. Chem.* **272**, 30455–30462.
30. Frangos, J. A., Eskin, S. G., McIntire, L. V. & Ives, C. L. (1985) *Science* **227**, 1477–1479.
31. Ridley, A. J. & Hall, A. (1992) *Cell* **70**, 389–399.
32. Smilenov, L. B., Mikhailov, A., Pelham, R. J., Marcantonio, E. E. & Gundersen, G. G. (1999) *Science* **286**, 1172–1174.
33. Schmid-Schönbein, G. W., Kosawada, T., Skalak, R. & Chien, S. (1995) *J. Biomech. Eng.* **117**, 171–178.
34. Haidekker, M. A., L'Heureux, N. & Frangos, J. A. (2000) *Am. J. Physiol.* **278**, H1401–H1406.
35. Butler, P. J., Norwich, G., Weinbaum, S. & Chien, S. (2001) *Am. J. Physiol.* **280**, C962–C969.
36. Jalali, S., del Pozo, M. A., Chen, K., Miao, H., Li, Y., Schwartz, M. A., Shyy, J. Y. & Chien, S. (2001) *Proc. Natl. Acad. Sci. USA* **98**, 1042–1046.
37. Tzima, E., del Pozo, M. A., Shattil, S. J., Chien, S. & Schwartz, M. A. (2001) *EMBO J.* **20**, 4639–4647.
38. Regen, C. M. & Horwitz, A. F. (1992) *J. Cell Biol.* **119**, 1347–1359.
39. Palecek, S. P., Schmidt, C. E., Lauffenburger, D. A. & Horwitz, A. F. (1996) *J. Cell Sci.* **109**, 941–952.
40. Ariyoshi, H., Yoshikawa, N., Aono, Y., Tsuji, Y., Ueda, A., Tokunaga, M., Sakon, M. & Monden, M. (2001) *J. Cell Biochem.* **81**, 184–192.
41. Ilic, D., Furuta, Y., Kanazawa, S., Takeda, N., Sobue, K., Nakatsuji, N., Nomura, S., Fujimoto, J., Okada, M. & Yamamoto, T. (1995) *Nature (London)* **377**, 539–544.
42. Sieg, D. J., Ilic, D., Jones, K. C., Damsky, C. H., Hunter, T. & Schlaepfer, D. D. (1998) *EMBO J.* **17**, 5933–5947.
43. Usami, S., Wung, S. L., Skierczynski, B. A., Skalak, R. & Chien, S. (1992) *Biophys. J.* **63**, 1663–1666.
44. Davies, P. F., Robotewskyj, A. & Griem, M. L. (1994) *J. Clin. Invest.* **93**, 2031–2038.
45. Girard, P. R. & Nerem, R. M. (1995) *J. Cell Physiol.* **163**, 179–193.
46. Franke, R. P., Grafe, M., Schnittler, H., Seiffge, D., Mittermayer, C. & Drenckhahn, D. (1984) *Nature (London)* **307**, 648–649.
47. Galbraith, C. G., Skalak, R. & Chien, S. (1998) *Cell Motil. Cytoskeleton* **40**, 317–330.